Electronic Supplementary Material (ESI) for Journal of Materials Chemistry

Supporting Information for

3D porous and redox-active prussian blue-in-graphene aerogels for highly efficient electrochemical detection of H_2O_2

*Liang Chen, xiaojuan Wang, Xuetong Zhang** and *huimin Zhang**

School of Materials Science & Engineering, Beijing Institute of Technology, Beijing 100081, P. R. China.

School of Chemistry, Beijing Institute of Technology, Beijing, 100081, P. R. China

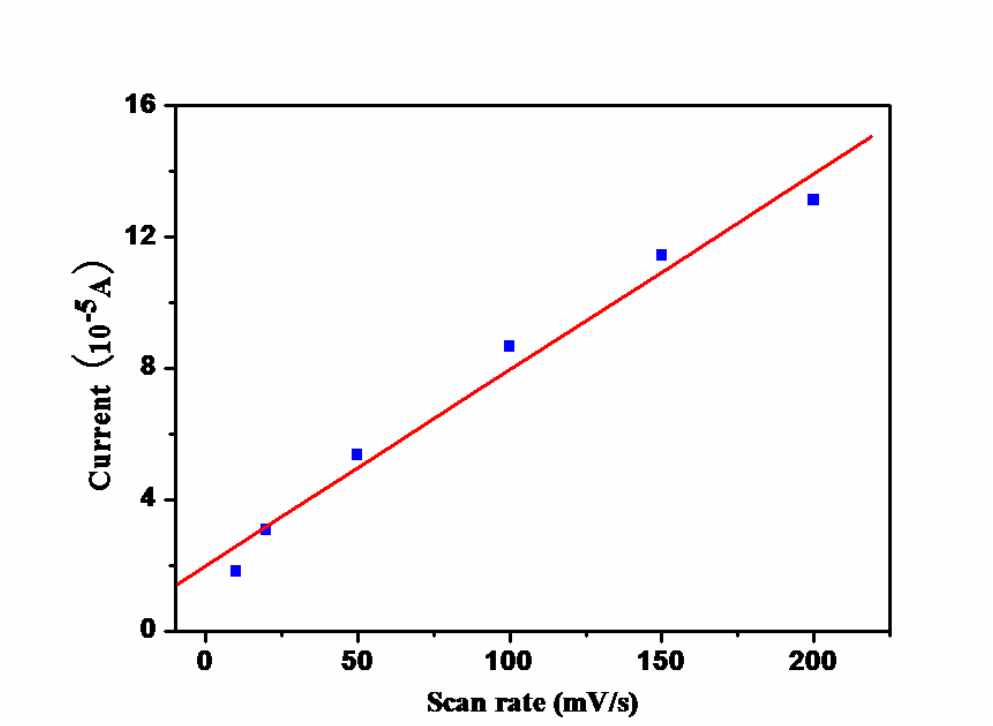

Fig. SI1 Plot of peak current versus scan rate for PB@G aerogel modified electrode

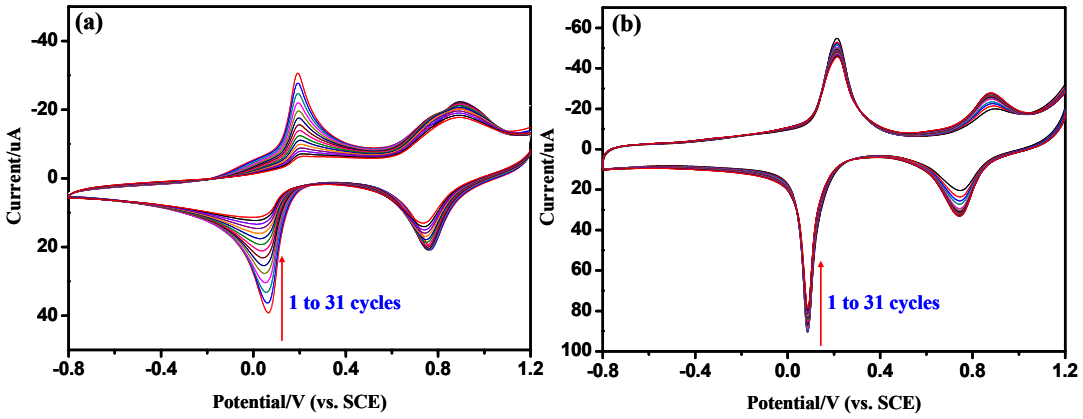

Fig. SI2. Cyclic voltammetry profiles of both PB powder (a) and PB@G aerogel (b) modified electrodes in 0.1 M PBS aqueous solution (pH = 7) at a scan rate of 50 mV s^{-1} (Only odd cycles were shown for clarity).

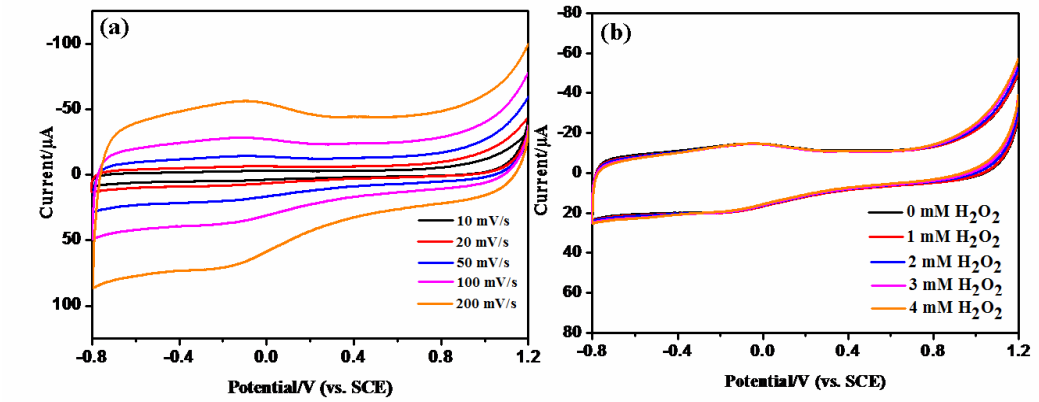

Fig. SI3 (a) Cyclic voltammetry of the pure graphene aerogel modified electrode at a scan rate of 10, 20, 50, 100, 150 and 200 mV s^{-1} and (b) cyclic voltammetry of graphene aerogel modified electrode with addition of different concentration of H_2O_2. The CV curve of graphene aerogel modified electrode presents a typical irregular rectangular shape and no obvious redox peaks were observed in comparison with that of the PB@G aerogel modified electrode. With addition of different concentration of H_2O_2, no apparent reduction peak can be observed, implying that the graphene aerogel can't electro-catalyze the reduction of H_2O_2.

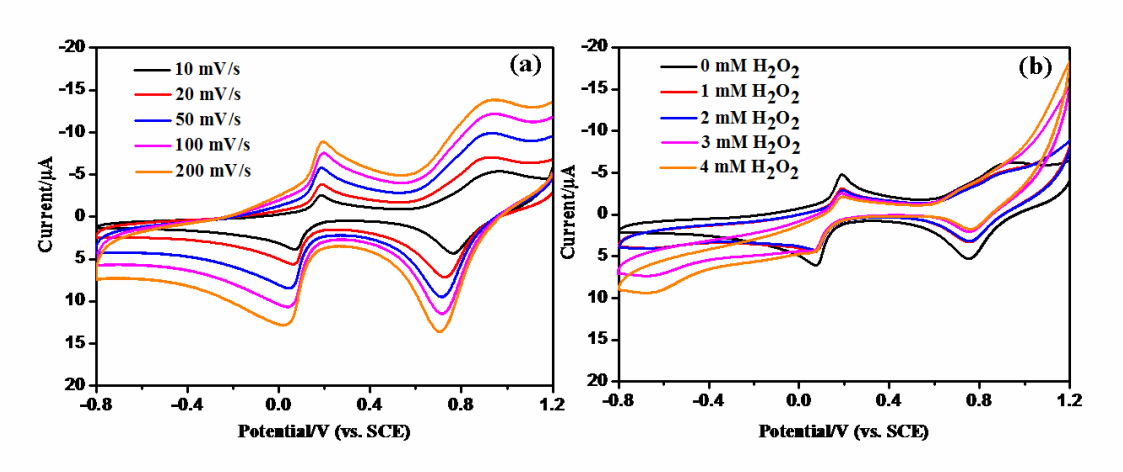

Fig. SI4. (a) Cyclic voltammetry of the PB powder modified electrode at a scan rate of 10, 20, 50, 100, 150 and 200 mV s^{-1} and (b) cyclic voltammetry of PB powder modified electrode with addition of different concentration of H_2O_2. An apparent reduction peak centered at -0.60 V can be observed from (b), which is much lower than that of PB@G aerogel modified electrode.

Table SI1 Porous attribute of the resulting PB@G aerogels with different mass ratios of graphene to PB.

Sample ID	**PB@G-1**	**PB@G-2**	**PB@G-3**
Graphene wt.%	71.4	50.0	28.6
BET area ($m^2\ g^{-1}$)	601	543	316
Pore volume ($cm^3\ g^{-1}$)	3.751	3.669	1.348
Pore size (nm)	25	27	17
Density ($mg\ cm^{-3}$)	45 ± 2	57 ±2	60 ±2

Table SI2 Performance comparison table of various electrodes in electrochemical detection of H_2O_2

Electrode	Limit of detection	Linear range	Reference
PB@G aerogel	0.005 μM	0.005 ~ 4 mM	Our work
PB/rGO	0.045 μM	5×10^{-5} ~ 0.12 mM	ACS Appl. Mater. Interfaces, 2010, 2 (8), 2339–2346
PB-graphene	7 μM	0.01 ~ 1.44 mM	Talanta, 15 (2011) 76-81
GO/PB	0.122 μM	0.0005 ~ 1.2 mM	Electrochimica Acta 56 (2011) 1239–1245
MCNT/PB	0.02 μM	0.0005 ~0.03 mM	Adv. Funct. Mater. 2009, 19, 3980–3986
PG/MWNTs/PB	1 μM	0.001 ~ 5 mM	Journal of Electroanalytical Chemistry 603 (2007) 59–66
PB–MWCNT/Au	0.023 μM	0.001 ~ 5 mM	J. Mater. Chem., 2010, 20, 1532–1537
PB-MCNT	0.567 μM	0.01 ~ 0.4 mM	Electroanalysis, 2009, 21,20, 2207-2212
CNTs/PB	≈ 0.005 μM	5×10^{-4} ~ 3×10^{-3}mM	J. Mater. Chem., 2012,22, 1824-1833
MWCNTs/Ag/PB	0.04 μM	8×10^{-5} ~ 5 mM	Anal. Sci., 2010, 26, 343
MWCNT/PVP/PB	0.025 μM	---	Adv. Funct. Mater. 2007, 17, 1574–1580
CNT/AuNPs/PB	3.36 μM	0.004 ~ 0.019 mM	Microchim Acta 2009, 167, 167-172
PB/OMC	1 μM	0.1 ~ 1.5 mM	Microporous and Mesoporous Materials 119 (2009) 193–199
Glutamate oxidase/PB	0.1 μM	10^{-4}~0.1 mM	Anal. Chem. 2000, 72, 1720-1723
PB Nanoelectrode	0.01 μM	10^{-5} ~ 10 mM	Anal. Chem. 2004, 76, 474-478
PBNPs/Nafion	1 μM	0.002 ~ 0.14 mM	Sensors and Actuators B 147 (2010) 270–276
thionin/EDTA/CNT/chitosan	0.065 μM	2×10^{-4}~8.5×10^{-2} mM	Microchim Acta (2010) 171:139–144
CNT/SCN	0.3 μM	5×10^{-4} ~ 1.67 mM	Chem. Mater. 2009, 21, 2247–2257
PNEGHNs	0.08 μM	0.001 ~ 0.5 mM	ACS Nano, 2010, 4 (7), 3959–3968
MWCNTs/TIi	0.38 μM	0.02 ~ 0.16 mM	Electroanalysis19 (2007) 1100–1108
CNTs/CB	10 μM	0.1 ~ 1 mM	Electroanalysis 20 (2008) 1788–1797
N-doped CNT	0.37 μM	1.76×10^{-3} ~ 0.139 mM	ACS Nano, 2010, 4 (7), 4292–4298
HRP/sulfonated-G	1.17 μM	3.5×10^{-3} ~ 0.329 mM	Electroanalysis 2011, 23, No. 4, 900 – 906
MWNTs–PANI	0.005 μM	8×10^{-6} ~ 5×10^{-3} mM	Talanta 72 (2007) 437–442
PNEGHNs	0.08 μM	0.001 ~ 0.5 mM	ACS Nano, 2010,7,3959-3968
HRP/GMA-co-VFc	2.6 μM	2.0 ~ 30 mM	Sensors and Actuators B 145 (2010) 444–450
HI-ePt	4.5 μM	0.02 ~ 40 mM	Anal. Chem. 2002, 74, 1322-1326
HRP–Fe_3O_4/m-silica	0.43 μM	0.002 ~ 0.024 mM	J. Mater. Chem., 2010, 20, 5030–5034
BiHCF nanoplates	0.07 μM	6×10^{-4} ~ 0.2 mM	J. Phys. Chem. C 112 (2008) 7617–7623
Nf/CuO/Pt	0.06 μM	1.5×10^{-4}~9 mM	Journal of Electroanalytical Chemistry 612 (2008) 157–163
Hb/TiO_2 NP/PG	0.2 μM	0.009 ~ 0.1 mM	Anal. Chem. 2005, 77, 6102-6104
Nafion/HRP/TN-3/ITO	0.18 μM	0.001 ~ 0.78 mM	J. Mater. Chem., 2012, 22, 9019–9026
HRP/FeMeOH	2.5 μM	0.1 ~ 1.5 mM	Adv. Mater. 2010, 22, 2809–2813
HRP–GSs	0.1 μM	0.001 ~ 2.6 mM	Adv. Funct. Mater. 2010, 20, 3366–3372
SBP	0.5 μM	5×10^{-4} ~ 3×10^{-3} mM	Anal. Chem. 1999, 71, 1935-1939